Insulin–Metal Ion Interactions: The Binding of Divalent Cations to Insulin Hexamers and Tetramers and the Assembly of Insulin Hexamers†

Frederick D. Coffman‡ and Michael F. Dunn*

Department of Biochemistry, University of California at Riverside, Riverside, California 92521

Received December 17, 1987; Revised Manuscript Received March 25, 1988

ABSTRACT: An insulin hexamer containing one B10-bound Co(III) ion and one unoccupied B10 site has been synthesized. The properties of the monosubstituted hexamer show that occupancy of only one B10 site by Co^{3+} is sufficient to stabilize the hexameric form under the conditions of pH and concentration used in these studies. The experimentally determined, second-order rate constants for the binding of Zn^{2+} and Co^{2+} to the unoccupied B10 site are consistent with literature rate constants for the rate of association of these divalent metal ions with similar small molecule ligands. These findings indicate that the rate-limiting steps for Zn^{2+} and Co^{2+} binding involve the removal of the first aqua ligand. The rate constant for the binding of Cd^{2+} is significantly lower than the literature values for small molecule chelators, which suggests that some other protein-related process is rate-limiting for Cd^{2+} binding to the unoccupied, preformed B10 site. The kinetics of the assembly of insulin in the presence of limiting metal ion provides strong evidence indicating that the B13 site of the tetramer species can bind Zn^{2+}, Cd^{2+}, or Ca^{2+} prior to hexamer formation and that such binding assists hexamer formation. Both the tetramer and the hexamer B13 sites were found to exhibit similar affinities for Zn^{2+} and Cd^{2+} ($K_d \simeq 9$ μM), whereas the tetramer B13 sites bind Ca^{2+} much more weakly ($K_d \simeq 1$ mM for tetramer vs 83 μM for hexamer). The second-order rate constants estimated for the association of Zn^{2+} and Cd^{2+} to the tetrameric site indicate that the loss of the first inner-sphere aqua ligand is the rate-limiting step for binding.

The two-zinc insulin hexamer is one of the most thoroughly studied proteins. The independently determined high-resolution crystal structures of this aggregate form (Blundell et al., 1972; Peking Insulin Structure Research Group, 1974; Sakabe et al., 1981; Dodson et al., 1979; Bentley et al., 1976; Smith et al., 1984; Baker et al., 1988) make possible the correlation of results from a vast number of physical/chemical studies including NMR,[1] EPR, CD, centrifugation, light scattering, fluroescence, and UV–visible spectroscopy (Bradbury et al., 1981; Williamson & Williams, 1979; Sudmeier et al., 1981; Dunn et al., 1987; Palmieri et al., 1988; Frank et al., 1972; Frank & Veros, 1970; Fredericq, 1956; Goldman & Carpenter, 1974; Grant & Coombs, 1972; Jeffrey & Coates, 1966; Lord et al., 1973; Milthrope et al., 1977; Pocker & Biswas, 1980; 1981; Bohidar & Geissler, 1984; Strazza et al., 1985; Storm & Dunn, 1985; Kaarsholm & Dunn, 1987). In the crystal, zinc ions bind to two identical high-affinity sites located on the three-fold symmetry axis near each end of the hexamer. Liganding at each site involves three B10 histidyl imidazole rings and three water molecules which form a slightly distorted octahedral array (Blundell et al., 1972; Baker et al., 1988). The affinity of this site for zinc has been estimated to be approximately 1×10^9 M^{-1} (Brill & Venable, 1968). A number of transition metal ions, including Co^{2+}, Co^{3+}, Cd^{2+}, Fe^{2+}, Cu^{2+}, Ni^{2+}, and Mn^{2+} have been substituted for Zn^{2+} at this site in vitro (Schlictkrull, 1956; Blundell et al., 1972; Sudmeier et al., 1981; Storm & Dunn, 1985; Palmieri et al., 1988). Since each His(B10) site involves three histidines, one from each dimer, metal occupancy of both hexameric B10 sites links the six insulin monomers as two interdigitated trimers. The importance of this site to the structure and function of the insulin hexamer is underscored by the invariant occurrence of histidine at the B10 position in the insulins of nearly all higher vertebrates.

It has recently been reported that a third high-affinity metal-binding site is located near the center of the hexamer (Sudmeier et al., 1981; Emdin et al., 1980; Storm & Dunn, 1985; Dunn et al., 1987), where the six B13 glutamate carboxyl groups are positioned within a cavity about 12 Å in diameter (Figure 1). At pH 6.2 in the absence of a bound metal ion, the B13 carboxyl pairs within each dimeric unit of the hexamer are quite close to each other (Blundell et al., 1972; Baker et al., 1988). The two closest oxygen atoms are 2.5 Å apart, indicating these atoms share a hydrogen-bonded proton. Electron density maps of insulin crystals soaked with Zn^{2+}, Cd^{2+}, and Pb^{2+} show that these metals bind both to the His B10 and the Glu B13 sites (Emdin et al., 1980 Dunn et al., 1987; C. Hill, Z. Dauter, M. F. Dunn, and G. G. Dodson, unpublished results). Within the B13 cavity, cadmium and zinc bind to three positions located on the dimer–dimer pseudotwofold axes several angstroms from the threefold axis and approximately 3.5 Å apart. In the lead structure, the three sites are located approximately 5 Å apart and further away from the threefold axis. Each metal-coordinated B13 site is made from the two closest carboxyl groups from adjacent dimers. Consequently, the hydrogen bonds between Glu(B13)

†Supported by NIH Grant AM31138BMT and by the Southern California Affiliate of the American Diabetes Association.

* To whom correspondence should be addressed.

‡Present address: Department of Pathology, Hahnemann University, Philadelphia, PA 19102-1192.

[1] Abbreviations: NMR, nuclear magnetic resonance; In, insulin; 2Zn–insulin, crystalline form of the insulin hexamer containing 2 Zn^{2+}/hexamer, occupying the His(B10) sites; 4Zn–insulin, crystalline form of hexamer obtained in the presence of high salt concentrations containing four relatively high affinity zinc ion sites (albeit only partially occupied); PB model, model for aggregation of metal-free insulin proposed by Pocker and Biswas (1980, 1981); MUX, murexide; PIPES, piperazine-*N*,*N*′-bis(2-ethanesulfonic acid); Tris, tris(hydroxymethyl)-aminomethane; EDTA, ethylenediaminetetraacetic acid; M^{2+}, metal ion.

0006-2960/88/0427-6179$01.50/0

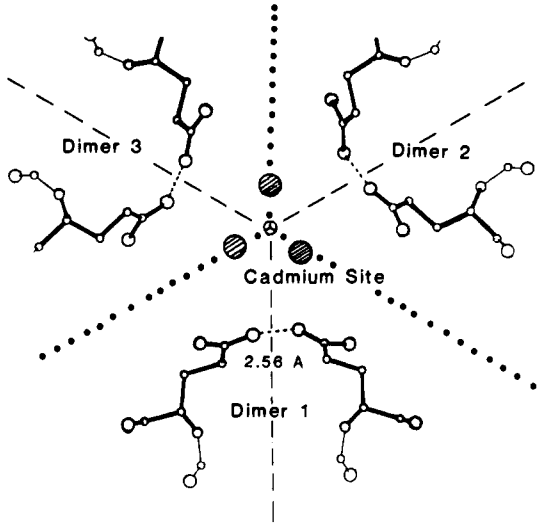

FIGURE 1: View along the threefold symmetry axis at the center of the 2Zn–insulin hexamer showing the positions of the Glu(B13) carboxyl groups prior to metal ion binding. Monomer–monomer interfaces (---); dimer–dimer interfaces (···). The distance between closest oxygen atoms across the monomer–monomer interface (2.5 Å) indicates each pair is hydrogen bonded. The cross-hatched circles located on the dimer–dimer interfaces indicate the positions of Cd^{2+} ions located in the X-ray structure of the 3Cd–insulin hexamer (Dunn et al., 1987). The electron density maps indicate a disordered structure in which the B13 carboxyl groups change position such that each Cd^{2+} site is formed by two carboxylates, one from each dimer. The Cd^{2+} occupancy at each site is approximately one-third. Hence, the two carboxyl groups closest to each cadmium position rearrange to form a dicarboxylate cage that stabilizes the hexamer, and the H bonds between those carboxyls and their intradimer partners are broken. Structure redrawn from graphic courtesy of G. Dodson.

pairs of the 2Zn hexamer which bridge the monomer–monomer interface reorient to form a divalent metal-binding site across the dimer–dimer interface. Equilibrium dialysis and NMR experiments show that calcium behaves like cadmium; Ca^{2+} competes with Cd^{2+} for the B13 site, and only one Ca^{2+} binds per hexamer (Sudmeier et al., 1981; Storm & Dunn, 1985; Dunn et al., 1987). Since the B13 site is located between dimers, and since this site exists both in the tetrameric and hexameric insulin species (but not in the dimer), binding to this site must play a role in stabilizing tetramer and hexamer.

In contrast to Ca^{2+} and Cd^{2+}, Co^{2+} has very low affinity for the B13 site (Sudmeier et al., 1981; Storm & Dunn, 1985; Roy et al., 1987). ^{113}Cd NMR studies (Sudmeier et al., 1981) show that Co^{2+} does not displace B13-bound $^{113}Cd^{2+}$, even at high concentrations of Co^{2+}. Equilibrium binding studies establish a stoichiometry of 2 Co^{2+}/6 insulin monomers over a wide range of cobalt concentrations, indicative of a marked preference for the B10 sites (Schlichtkrull, 1956; Brill & Venable, 1968; Storm & Dunn, 1985). Preliminary diffraction data show both Co^{2+} and Co^{3+} insulin crystals are nearly isomorphous with the 2Zn crystals (Z. Dauter, M. F. Dunn, and G. G. Dodson, unpublished results). Both Co^{2+} and Co^{3+} have weak visible absorbance bands arising from d–d transitions (with ϵ values of 50–150 M^{-1} cm^{-1}) that provide spectrophotometric signals which allow certain cobalt–insulin interactions to be followed (Storm & Dunn, 1985; Kaarsholm & Dunn, 1987; Dunn et al., 1987).

Due to the high activation energies associated with ligand exchange reactions, Co^{3+} complexes are termed "exchange inert". Insulin hexamers containing Co^{3+} at both B10 positions have been synthesized previously and used to characterize the binding of Ca^{2+} and Cd^{2+} to the B13 site of the insulin hexamer (Sudmeier et al., 1981; Storm & Dunn, 1985; Kaarsholm & Dunn, 1987). Since Co^{3+} hexamers do not dissociate, even at submicromolar concentrations, the Co^{3+}-substituted species may be used to study events unique to the hexameric state.

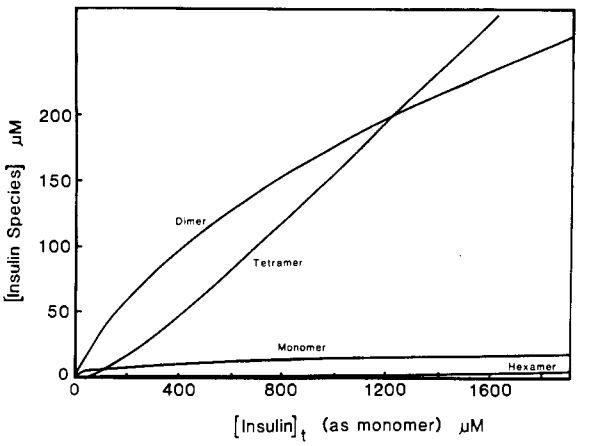

FIGURE 2: Distribution of the concentrations of metal-free insulin monomer, dimer, tetramer, and hexamer calculated from the association constants proposed by Pocker and Biswas (1980, 1981). Association constants: $K_{12} = 7.5 \times 10^5$ M^{-1}; $K_{24} = 5 \times 10^3$ M^{-1}; $K_{46} = 45$ M^{-1} (see eq 1–3, text). The concentrations of dimer and tetramer increase steeply, and these dependencies are roughly parallel, while the level of monomer increases only gradually and, with respect to the experiments described herein, is not a significant species at high total insulin concentrations. The amounts of metal-free hexamer present are always negligible in comparison to dimer and tetramer levels.

In the absence of divalent cations, insulin exists as a distribution of monomers, dimers, tetramers, hexamers, and hexamer aggregates [viz. Blundell et al. (1972) and Baker et al. (1988) and references cited therein]. At neutral pH and in the absence of divalent metal ions, ultracentrifugation and circular dichroism (CD) studies yield dimerization constants (K_{12}) in the range 1×10^5 to 2.2×10^5 M^{-1} (Strazza et al., 1985; Lord et al., 1973; Jeffrey et al., 1976; Rupley et al., 1967; Goldman & Carpenter, 1974). Using a sensitive UV difference circular dichroism technique which could measure spectral changes at 10^{-8} M insulin, Pocker and Biswas (1980, 1981)[2] found a larger apparent value for K_{12}, 7.5×10^5 M^{-1}. In each of the above-mentioned studies, the dependence of the average molecular weight on total insulin concentration was computer-fit to a variety of association models. In all cases, only those models that allowed even-numbered aggregates (i.e., dimers, tetramers, and hexamers, as shown in Scheme I) give reasonable fits to the experimental data.

Scheme I

$$2\mathrm{In} \underset{}{\overset{K_{12}}{\rightleftharpoons}} (\mathrm{In})_2 \quad (1)$$

$$2(\mathrm{In})_2 \overset{K_{24}}{\rightleftharpoons} (\mathrm{In})_4 \quad (2)$$

$$(\mathrm{In})_4 + (\mathrm{In})_2 \overset{K_{46}}{\rightleftharpoons} (\mathrm{In})_6 \quad (3)$$

The equilibrium constants proposed by Pocker and Biswas (1980, 1981), $K_{12} = 7.5 \times 10^5$ M^{-1}, $K_{24} = 5 \times 10^3$ M^{-1}, and $K_{46} = 45$ M^{-1}, fit the available experimental data much more closely than any other values yet published. The allowed species, monomer, dimer, tetramer and hexamer (eq 1–3 of Scheme I) are consistent with inferences drawn from the X-ray structure, require no new modes of interaction, and minimize

[2] However, Kaplan et al. (1984) have suggested that this value may be in error due to surface adsorption of insulin on the cuvette windows.

nonproductive interactions to form odd aggregates.

The predicted molar distribution of subspecies is plotted against the total insulin concentration for the Pocker–Biswas model[3] (the PB model) in Figure 2. As the total insulin level rises, the dimer and tetramer populations increase far above the monomer and (barely discernible) hexamer populations. At the millimolar concentrations found in the cellular compartments where assembly occurs, the PB model predicts metal ion free insulin would exist primarily as dimers and tetramers;[4] hence, assembly of 2Zn–insulin hexamers requires only a bimolecular collision between the predominant species. Consequently, the PB model predicts species distributions that are compatible with the in vivo behavior of the hormone: insulin associates easily and cleanly into hexamers under conditions similar to that of the storage granule, and insulin dissociates under the conditions of dilution found in circulation.

In this study, we report a procedure for synthesizing insulin hexamers that contain only one Co^{3+} [bound to a His(B10) site], and these monosubstituted hexamers are used to study the binding of divalent cations to the unoccupied hexameric B10 site. The B10–metal association constants we report herein are used to identify B10-related kinetic processes when high levels of insulin are mixed with limiting amounts of Co^{2+}, Zn^{2+}, Cd^{2+}, or Ca^{2+}. The characteristic behavior of these time courses are consistent with a hexamer assembly model in which the first metal ion binding step involves the B13 site of metal-free insulin tetramer. This metal-coordinated tetramer then combines with a metal-free dimer to form a hexamer which rapidly takes up metal ions at the His-B10 sites.

Materials and Methods

Materials. Porcine zinc insulin was purchased from Elanco (Lilly). Murexide and 2,2′,2″-terpyridine were obtained from Sigma. Chelex 100 resin was obtained from Bio-Rad. All other chemicals are reagent grade. To remove metal contaminants, glassware was soaked for several days in 3 N HNO_3 and then rinsed with metal-free deionized–distilled water. Water was deionized and then distilled and stored in acid-washed glass containers.

Preparation of Metal-Free and Metal-Substituted Insulin Species. Commercial zinc insulin is made metal free by mixing 250 mg of the protein in 10 mL of H_2O, adjusting the mixture to pH 10.5 with 1 N NaOH to completely dissolve the protein, then adding 2 mL of hydrated Chelex 100 resin, and finally adjusting the pH to 8.7 with 1 N HCl. This preparation is allowed to stir at least 1 h and then centrifuged in acid-washed conical centrifuge tubes to pellet the resin. The supernatant is carefully removed and lyophilized and stored at −20 °C. Insulin solutions were prepared by weighing out and then dissolving the desired amount of lyophilized insulin in metal-free buffer to which the appropriate metal ions are then added.

Insulin concentrations are determined from the absorbance at 280 nm by using $\epsilon_{280} = 5.7 \times 10^3$ M^{-1} cm^{-1} (Porter, 1953). Terpyridine concentrations are determined at 290 nm, with $\epsilon = 1.6 \times 10^4$ M^{-1} cm^{-1} (Holyer et al., 1966). Concentrations of zinc, cobalt, and cadmium are determined via spectrophotometric titration of the complexes with terpyridine (terpy). The bis complex extinction coefficients are (in units of M^{-1} cm^{-1}): $Zn(terpy)_2$, $\epsilon_{333} = 3.78 \times 10^4$; $Co(terpy)_2$, $\epsilon_{330} = 2.58 \times 10^4$; $Cd(terpy)_2$, $\epsilon_{330} = 3.25 \times 10^4$.

Kinetic Studies. Rapid kinetic experiments were performed with a Durrum D-110 stopped-flow spectrophotometer. Kinetic time courses were collected by a menu-driven FORTRAN program on an IBM PC, converted to digital form, displayed, and stored on floppy disks for analysis. Time courses are plotted and fit to one, two, or three consecutive first-order (single exponential) events using a nonlinear least-squares algorithm. Software for data collection and analysis was written by M. F. Dunn, R. G. Morris, S. C. Koerber, J. Fluke, and J. Mason. Murexide experiments were performed by rapidly mixing buffered, metal ion free insulin with freshly prepared murexide–metal ion solutions and monitoring either the disappearance of the metal ion–murexide complex absorbance or the increase in the free murexide absorbance.

Synthesis of Monosubstituted Co^{3+} Hexamers. To a solution containing 150 μM metal ion free insulin is added a small volume of concentrated Zn^{2+}–Co^{2+} solution; after mixing, the reactant concentrations are $[Zn^{2+}] = 30$ μM and $[Co^{2+}] = 20$ μM. Following a 5-min incubation at room temperature, the solution is allowed to stand overnight at 4 °C in the presence of 20 mM H_2O_2 to oxidize Co^{2+} to Co^{3+}. Addition of 500 μM EDTA sequesters all Zn^{2+} and any residual Co^{2+}, and the mixture is immediately passed over a Sephadex G-100 column. The initial peak contains mono- and disubstituted Co^{3+} hexamers, while metal ion free insulin, excess EDTA, and the EDTA-complexed metal ions elute in later fractions. The hexamer-containing fractions are concentrated by using pressure dialysis until the solution is a rosy pink to red color [see Storm and Dunn (1985) for the spectrum of Co^{3+}-substituted insulin hexamer]. The concentration of occupied B10 sites is found by measuring the absorbance at 520 nm, where bound Co^{3+} has a small absorbance ($\epsilon = 150$ M^{-1} cm^{-1} per B10 site). The total protein is determined by diluting an aliquot of the concentrated hexamer fraction in buffer and measuring the absorbance at 280 nm. By comparing the total hexamer concentration to the concentration of occupied B10 sites, the concentration of monosubstituted species is found.

Results

Murexide Controls. From pH 6.6 to pH 9.0, the long-wavelength π,π^* transition of metal ion free MUX is centered at 520 nm with $\epsilon_{max} = 1.3 \times 10^4$ M^{-1} cm^{-1} (F. Coffman and J. Fluke, unpublished data). Depending upon the metal ion, the absorbance maxima of the MUX mono complexes are blue-shifted 35–65 nm, and the extinction coefficients of these complexes are 30–40% larger than that of metal ion free MUX. The spectrum of each metal ion–murexide system has two regions of large absorbance change, one near 460 nm from the appearance of the complex and one near 535 nm from disappearance of free murexide. Although the spectra remain the same as the ionic strength increases, the affinity of MUX for each metal ion decreases. For example, in 5 mM PIPES–NaOH at pH 7, the dissociation constant for Co^{2+} is 1.3×10^{-4} M. In 20 mM PIPES–NaOH, also at pH 7, it is

[3] A potential problem with this model is its manner of construction. The dimerization constant was obtained by Pocker and Biswas (1980, 1981) in 5 mM $KHPO_4$, pH 7, while the centrifugation data used to fit K_{24} and K_{46} were obtained by Goldman and Carpenter in 169 mM Tris-HCl, pH 8. In earlier sedimentation experiments where pH was varied, the weight-average molecular weight was found to decrease in a sigmoidal fashion as pH is increased from pH 7.4 to pH 9.5. However, as the change in weight-average molecular weight between pH 7 and pH 8 is not large, and the fit to the experimental data is so close compared to other models, we conclude that between pH 7 and pH 8 the PB model gives the best available description of the distribution of metal-free insulin species.

[4] The osmometry measurements of J. F. Hansen (Novo Research Institute, private communication) indicate that the PB model underestimates the amount of metal-free hexamer. However, Hansen's measurements concur with the conclusion that metal-free tetramer is a predominant species in the low millimolar range of insulin chains.

3.8×10^{-4} M. For the metal ions and experimental conditions used herein, MUX binds with dissociation constants between 10^{-3} M and 10^{-6} M, values far weaker than the 1×10^{-9} M value of the B10 site. The dissociation constants for metal–murexide complexes measured at pH 8 in 5 mM PIPES–NaOH buffer are as follows: Zn^{2+}, K_d = 60 μM; Co^{2+}, K_d = 130 μM; Cd^{2+}, K_d = 40 μM; Ca^{2+}, K_d = 800 μM.

Except for Co^{2+}, the rate constants for metal ion–murexide association and dissociation are extremely rapid, and under the conditions used in these studies, complex formation is complete in less than 3 ms (the instrument mixing dead time). The reaction of Co^{2+} with MUX exhibits association and dissociation rate constants that, in comparison with Zn^{2+}, Cd^{2+}, and Ca^{2+}, are relatively slow. Hence, an observable Co^{2+}–MUX relaxation is generated either by dilution of a murexide–metal ion solution with buffer or by the mixing of MUX with metal ion ($1/\tau \simeq 175$ s^{-1}). Both in rapid kinetic studies and in equilibrium experiments, no spectral changes are detected when MUX is mixed with metal ion free insulin (data not shown).

Binding of Zn^{2+}, Co^{2+}, and Cd^{2+} to Preformed Hexameric B10 Sites. As described under Materials and Methods, hexamers containing Co^{3+} coordinated to one B10 site but with no metal ion in the other B10 site were synthesized. Then in separate experiments, equal concentrations of dilute monosubstituted hexamer or metal ion free insulin were added to excess cadmium in the presence of MUX. The monosubstituted hexamers were found to bind approximately half as much cadmium per mole as six metal ion free insulin monomers (data not shown).

For kinetic experiments, solutions ranging from 2 to 5 μM total unoccupied B10 sites were prepared from a concentrated hexamer fraction. These solutions then were mixed (Figure 3) with an excess of either Zn^{2+} (A), Co^{2+} (B), or Cd^{2+} (C) in the presence of MUX. For those experiments where the concentration of unoccupied B10 sites is below 5 μM, a trace of EDTA was added to the protein stock solution to prevent prior occupancy of the B10 sites by small amounts of contaminating zinc. Neither the EDTA nor the disubstituted hexamers present in the sample were found to have any effect on the results; control experiments established that EDTA binding occurs within the instrument dead time, and the disubstituted hexamer has no available high-affinity binding sites for EDTA-coordinated metal ions.

The time courses were found to be adequately fit by the rate expression for a first-order relaxation:

$$A_t = A_{TOTAL}e^{-t/\tau} \quad (4)$$

where A_t is the absorbance change at time t, A_{TOTAL} is the total absorbance change, and τ is the relaxation time.

If binding is a single bimolecular reaction

$$(In)_6(Co^{3+})_1 + M^{2+} \underset{k_{-1}}{\overset{k_1}{\rightleftharpoons}} (In)_6(Co^{3+})_1(M^{2+})_1 \quad (5)$$

then the relaxation equation that applies to this system is given by

$$k_{obsd} = 1/\tau_1 = k_1(A' + B') + k_{-1} \quad (6)$$

where A' and B' represent the concentrations of the free species $(In)_6(Co^{3+})_1$ and M^{2+} after the relaxation, k_1 is the second-order rate constant for complex formation, and k_{-1} is the unimolecular rate constant for dissociation of metal ion from the site. Under conditions where the metal ion concentration is in large excess over $(In)_6(Co^{3+})_1$ and k_{-1} is small, eq 6 simplifies such that $1/\tau_1$ becomes proportional to $[M^{2+}]$:

$$1/\tau_1 = k_1[M^{2+}] \quad (7)$$

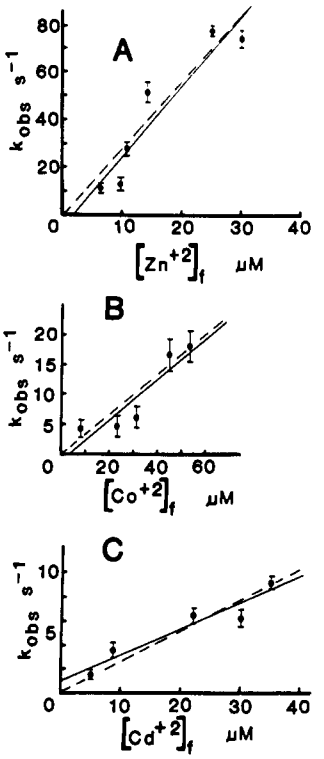

FIGURE 3: Kinetics of Zn^{2+} (A), Co^{2+} (B), and Cd^{2+} (C) binding to the preformed B10 site of the monosubstituted Co^{3+}–insulin hexamer. Dilute solutions of $(In)_6(Co^{3+})_1$ (2–5 μM unoccupied B10 sites) were mixed with excess Zn^{2+} (A), Co^{2+} (B), and Cd^{2+} (C) in the presence of MUX (20 μM) at pH 7.8 in 20 mM Tris-HCl at 25.0 ± 0.2 °C. The observed rates of metal ion binding (measured as the disappearance of murexide–metal ion complex; see Materials and Methods) are plotted vs the final concentration of free metal ion. The formation rate constants (slopes of the plots) for binding to a hexameric B10 site are as follows: Zn^{2+}, $k_1 = 2.9 \times 10^6$ M^{-1} s^{-1}; Co^{2+}, $k_1 = 3.5 \times 10^5$ M^{-1} s^{-1}; Cd^{2+}, $k_1 = 2.2 \times 10^5$ M^{-1} s^{-1}.

When the observed rates are plotted against free metal ion concentration (Figure 3), the points fall on lines which, within experimental error, pass through the origin (the slopes and intercepts of the lines are drawn from the best-fit least-squares analysis). Thus, the k_{-1} values must be very small. The following formation rate constants (k_1) were obtained: Zn^{2+}, $k_1 = 2.9 \times 10^6$ M^{-1} s^{-1} (A); Co^{2+}, $k_1 = 3.5 \times 10^5$ M^{-1} s^{-1} (B); Cd^{2+}, $k_1 = 2.2 \times 10^5$ M^{-1} s^{-1} (C). These rate constants are not changed significantly when the lines drawn through the data points are constrained to pass through the origin (viz., the dashed lines in Figure 3).

Assembly of Insulin Oligomers When Insulin Is in Excess of Metal Ion. To examine the assembly of insulin with other divalent cations, experiments were carried out (Figure 4) wherein a large excess of metal ion free insulin is mixed with limiting amounts of either Zn^{2+} (A), Co^{2+} (B), Cd^{2+} (C), or Ca^{2+} (D) in the presence of MUX. In the experiments with Zn^{2+}, Co^{2+}, or Cd^{2+}, 1.23 mM metal ion free insulin was mixed with 40 μM metal ion in 5 mM PIPES–NaOH buffer, pH 7.0. Since the interaction between metal ion free insulin and Ca^{2+} is relatively weak (Storm & Dunn, 1985), 500 μM Ca^{2+} was used. At 1.23 mM, total insulin concentration, the PB model predicts the distribution of subspecies to be [dimer] $\simeq$ [tetramer] $\simeq$ 200 μM, while the predicted levels of monomer (15 μM) and metal ion free hexamer (2 μM) should be negligible. If all dimer and tetramer initially present is converted to hexamer upon reaction, then 40 μM metal ion represents 10% of the total hexameric B10 sites.

Representative time courses are displayed in Figure 4. The outstanding qualitative result of this experiment is the dramatic

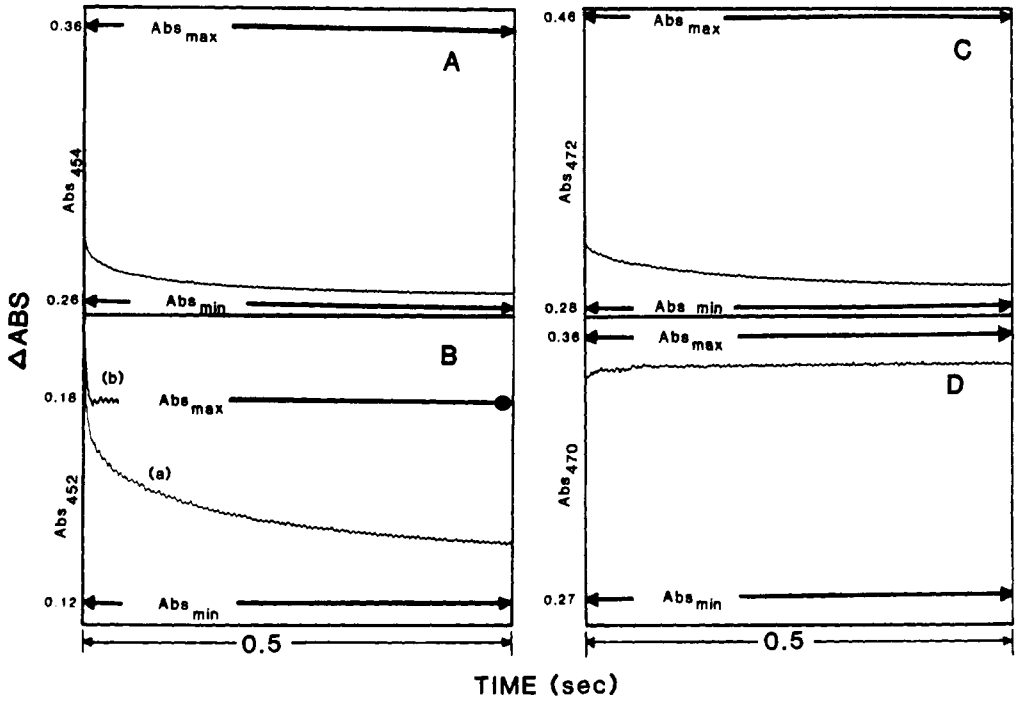

FIGURE 4: Single-wavelength stopped-flow time courses for the uptake of Zn^{2+} (A), Co^{2+} (B), Cd^{2+} (C), and Ca^{2+} (D) when the respective metal ion–murexide complexes are mixed with a high concentration of metal-free insulin. Conditions after mixing: [insulin as monomer] = 1.23 mM; [MUX] = 20 μM; (A) [Zn^{2+}] = 40 μM, (B) [Co^{2+}] = 40 μM, (C) [Cd^{2+}] = 40 μM, or (D) [Ca^{2+}] = 500 μM; 5 mM PIPES–NaOH buffer, pH 7.0 at 25.0 ± 0.2 °C. Note the large changes in absorbance that occur within the mixing dead time for the Zn^{2+} (85%), Cd^{2+} (85%), and Ca^{2+} (10–15%) systems. Very little (if any) Co^{2+} is bound in the dead time. The fast relaxation in the Co^{2+} time courses (traces a and b) is a Co^{2+}–MUX relaxation due to dilution (see text). The indicated maximum and minimum absorbance values are controls measured in the absence of insulin for the metal ion–MUX complexes mixed respectively with buffer and with EDTA.

loss of absorbance in the mixing dead time observed in the experiments with zinc (A), cadmium (C), and calcium ions (D). Approximately 80–85% of the total amount of Zn^{2+} or Cd^{2+} is consumed by this event. In the Ca^{2+} experiment (Figure 4D), approximately 10–15% of the total Ca^{2+} is bound in the mixing dead time, an amount that corresponds to 50–75 μM of the 500 μM total, but no further binding was observed. However, very little, if any, Co^{2+} is bound in the mixing dead time (Figure 4B).

Figure 4B shows the time course (trace a) for the uptake of Co^{2+}. There is a rapid initial decrease in the MUX–Co^{2+} signal which is complete in the first 15 ms. This fast relaxation is followed by a slower rate of uptake which consists of at least two relaxations. Trace b is a control experiment in which the same MUX–Co^{2+} solution is mixed with buffer. Note that the rapid relaxation due to dilution of the complex has an amplitude that is only slightly smaller than the amplitude of the fast relaxation in trace a. When the amplitude of the relaxation due to dilution (trace b) is subtracted from the fast relaxation in trace a, it is apparent that no more than 2–4 μM Co^{2+} could have been taken up by insulin in the rapid phase.

Table I presents a summary of the dead-time binding events, the known major site preferences for each metal, and the predicted concentrations of species containing these sites. If the PB model predicts the qualitative distribution of metal ion free insulin species correctly, then it is obvious that preexisting metal ion free hexamer cannot account for much of the dead-time binding. There is simply not enough metal ion free hexamer present. Rapid assembly followed by rapid metal ion binding to the B10 sites cannot be responsible for this event either. The association rate constant for cadmium binding to the B10 site (viz. Figure 3) predicts that Cd^{2+} should bind somewhat slower than Co^{2+}, whereas Figure 4 shows Cd^{2+} binds much faster. In fact, given the association rate constants for the binding of these three divalent cations to a preformed

Table I: Summary of Dead-Time Metal Ion Binding to 1.23 mM Insulin

metal ion	metal ion bound in dead time/ total metal ion	binding sites	potential binding species
Zn^{2+}	34 μM bound/ 40 μM total	B10, B13	hexamer (2 μM), tetramer (200 μM)
Co^{2+}	<5 μM bound/ 40 μM total	B10	hexamer (2 μM)
Cd^{2+}	34 μM bound/ 40 μM total	B10, B13	hexamer (2 μM), tetramer (200 μM)
Ca^{2+}	60 μM bound/ 500 μM total	B13	tetramer (200 μM)

His(B10) site (Figure 3), no single hexamer concentration can satisfactorily predict the kinetic behavior seen for these three metal ions. Further, Ca^{2+}, which does not bind to hexameric B10 sites, is also bound in an extremely rapid step. These observations indicate that the dead-time changes cannot be the consequence of binding to preformed or rapidly assembled B10 sites. Most likely these rapid events result from binding to preformed sites other than the hexameric B10 site, while the slower uptake of metal ion is the result of the rate-limiting assembly of dimers and tetramers to form competent hexamers. Therefore, the dead-time absorbance losses must be due to some other site that preexists on the insulin dimer and/or the insulin tetramer. Since the most likely site available is the Glu(B13) site of the insulin tetramer (see Discussion), the following experiments were carried out.

To study the binding of Zn^{2+} and Cd^{2+} to the B13 sites on the tetramer, either 40 μM Zn^{2+} or 40 μM Cd^{2+} was mixed with various concentrations of metal-free insulin in the presence of MUX. Since the extinction coefficients of free MUX and these metal–MUX complexes are known, and provided quasi-equilibrium has been reached between the available metal ion and the two competing chelators (i.e., MUX and the B13

site), the concentrations of these species at the end of the dead-time binding event can be found by using

$$A = \epsilon_{complex}([MUX]_0 - [MUX]_f) + \epsilon_{MUX}[MUX]_f \quad (8)$$

where A is absorbancy and the subscripts "0" and "f" refer to total and free concentrations, respectively. Because the concentrations and dissociation constants of all MUX species are known, the dissociation constant of the B13 site can be estimated from the following relationships: (1) The concentration of free metal after dead-time binding is given by

$$[M]_f = K_d^*[MUX-M]/[MUX]_f \quad (9)$$

where MUX–M is the MUX–metal ion complex. (2) The total metal bound in the mixing dead-time binding event = $[M]_b$, where

$$[M]_b = [M]_0 - ([M]_f + [MUX-M]) \quad (10)$$

(3) The concentration of free B13 sites = $[B13]_0 - [M]_b$ (subscript "b" denotes bound metal ion), where $[B13]_0 = [(In)_4]_0$ (from the PB model) and [B13–M] = $[M]_b$. (4) Then the dissociation constant of the B13 site can be calculated from the relationship

$$K_d = ([B13]_f[M]_f)/[B13-M] \quad (11)$$

Dissociation constants for zinc and cadmium derived from the experimentally determined stopped-flow amplitudes are plotted against the total tetramer concentration at various total insulin concentrations in Figure 5A. Both metal ions bind with approximately the same affinity, $K_d = 9 \times 10^{-6}$ M. Note that if the above calculations are performed with the assumption that dimer is the binding species, then the calculated K_d values span several orders of magnitude. Therefore, these results strongly support the identification of the dominant dead-time event as binding to the B13 sites of the tetramer. The utility of the PB model as a predictor of the concentrations of metal ion free species over the range of insulin concentrations studied is also supported.

At several concentrations of insulin, the "tail end" of the process described herein as the "dead-time" event could be detected. Analysis of this time course makes possible estimation of the apparent rate constant as follows: with the assumption that the dead-time event is a single, pseudo-first-order process, both the total amplitude of the event and the absorbance change at each of the first six half-lives ($t_{1/2}$) can be estimated; therefore, the half-life, and thus the rate, can be estimated. For example, if one excepts the change in absorbance due to the dead-time event at the end of four half-lives to be 0.015 absorbance unit and this change is seen to occur in the time course at 4.5 ms after mixing, then the value of $t_{1/2}$ is approximately 4.5/4 = 1.13 ms, and the pseudo-first-order rate constant is approximately $0.693/(1.13 \times 10^{-3})$ $s^{-1} \simeq 600$ s^{-1}. With the assumption that this system is an A + B = C system, where A, B, and C represent free metal ion, free B13 species, and the B13–metal ion complex, respectively, then the relaxation expression for this system is also given by eq 4. According to eq 6, a plot of observed rate vs free ligand concentration will be linear with slope = k_1 and y intercept = k_{-1}.

These plots are shown in Figure 5B. The specific association rate constants (k_1) estimated for both metals are fast. Zinc has an association rate, k_1, of $\sim 5 \times 10^6$ M^{-1} s^{-1} and a y intercept (k_{-1}) of ~ 270 s^{-1}, whereas cadmium has values of $k_1 \sim 9 \times 10^6$ M^{-1} s^{-1} and $k_{-1} \sim 140$ s^{-1}. These values are consistent with literature values for the binding of small molecule ligands to Zn^{2+} and Cd^{2+}. The dissociation constants,

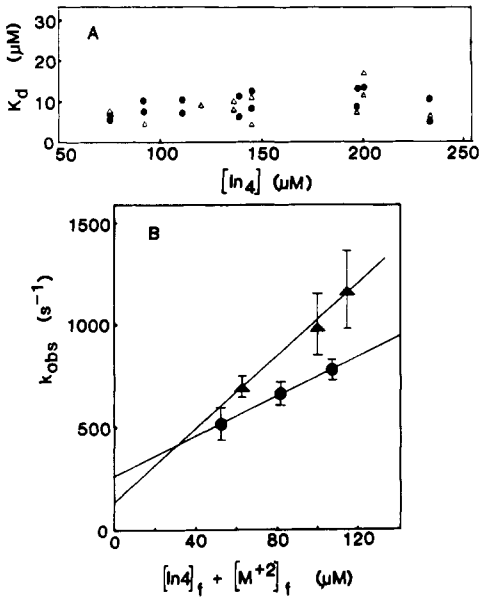

FIGURE 5: Binding of Zn^{2+} and Cd^{2+} to tetramer B13 sites. (A) The amount of tetramer predicted by the Pocker–Biswas model (PB model; see introduction) is plotted vs the apparent dissociation constants estimated from amplitudes measured as the "dead-time" loss of absorbance (viz., Figure 4) for the reaction of Zn^{2+} (●) and Cd^{2+} (△) with different concentrations of metal-free insulin. The concentration change of the dead-time binding event was calculated from known extinction coefficients and MUX–metal ion binding constants (see text). The consistency of the Zn^{2+} and Cd^{2+} dissociation constants (8.5 μM and 9.6 μM, respectively) indicates the PB model is valid over the wide range of insulin concentrations used. Concentrations after mixing: $[Zn^{2+}] = 40$ μM; $[Cd^{2+}] = 40$ μM; [MUX] = 20 μM; [insulin] varied from 300 μM to 2 mM (as monomer); 20 mM Tris-HCl buffer, pH 7.6 at 25.0 ± 0.2 °C. (B) Estimation of the Zn^{2+} (●) and Cd^{2+} (▲) association rate constants from single-wavelength stopped-flow time courses. The reactions of Zn^{2+} and Cd^{2+} with excess metal-free insulin in 20 mM Tris-HClbuffer, pH 7.6, are nearly too fast to be measured via stopped-flow methods (viz., Figure 4). However, the tail end of the dead-time binding event can be observed at the lower insulin concentrations, and crude values of the apparent rate constant (assuming the dead-time change is a pseudo-first-order process) could be estimated from the estimated half-lives of these reactions. These rate values are plotted vs the sum of the free metal ion and free tetramer concentrations (see text). The slope of the best-fit, solid line drawn through each data set provides an estimate of k_1, while the y intercept provides an estimate of k_{-1}. These values for Zn^{2+} are $k_1 \simeq 5 \times 10^6$ M^{-1} s^{-1} and $k_{-1} \simeq 270$ s^{-1}, and for Cd^{2+} they are $k_1 \simeq 9 \times 10^5$ M^{-1} s^{-1} and $k^{-1} \simeq 140$ s^{-1}.

calculated as $K_d = k_{-1}/k_1$, are $\sim 5.6 \times 10^{-5}$ M for Zn^{2+} and $\sim 1.5 \times 10^{-5}$ M for Cd^{2+}.

Discussion

Murexide Controls. The competing solution equilibria between MUX and insulin for metal ions are described by the equations:

$$\text{MUX} + \text{metal} \underset{k_{-m}}{\overset{k_m}{\rightleftharpoons}} \text{MUX–metal} \quad (12)$$

$$(\text{In})_n + \text{metal} \underset{k_{-1}}{\overset{k_1}{\rightleftharpoons}} (\text{In})_n\text{–metal} \quad (13)$$

Equation 12 describes the formation of complexes between MUX and metal ion, and eq 13 describes the formation of complexes between an insulin species (e.g., tetramer or hexamer) and metal ion. For MUX to function as an indicator, several criteria must be met. First, MUX cannot bind the metal ions with greater affinity than does insulin. Second, to ensure that the attainment of the MUX–metal ion equilibrium is not rate-limiting, k_m and k_{-m} must be fast relative to k_1 and

k_{-1}. Third, the concentration of MUX–metal ion complex must be small in comparison to the total metal concentration (Bernasconi, 1976). According to these criteria, MUX is a useful indicator for observing metal binding in the insulin assembly system. MUX binds the metal ions of interest much more weakly than does the hexamer B10 site. Metal ion binding is accompanied by large changes in the extinction coefficients of two wavelength regions, one near 460 nm, the other near 540 nm. These large spectral changes allow small changes in total metal concentration to be detected over the range of 10^{-6}–10^{-3} M total metal ion (the range over which the dissociation constants of the MUX–metal ion complexes allow the greatest sensitivity). With the exception of Co^{2+}, the half-lives for formation of MUX–metal ion complexes are fast relative to the mixing dead time. This result agrees with a literature value of <2 μs for the "relaxation time" of the Ca^{2+}–murexide complex (Scarpa et al., 1978). Since the zinc– and cadmium–MUX systems equilibrate essentially instantaneously to changing free metal concentrations, any *observed time course* must be due to metal ion binding processes involving insulin. In the case of Co^{2+}, the cobalt–MUX relaxation will be the observed, rate-limiting step for any insulin–Co^{2+} binding processes >200 s^{-1}, but for slower processes, especially those <20 s^{-1}, MUX also satisfies the requirements of a true indicator for detecting the concentration of Co^{2+} free in solution. In contrast to 4-(2-pyridylazo)resorcinol and 2,2′,2″-terpyridine, where Co^{2+}–chelator complexes rapidly and spontaneously oxidize to Co^{3+} complexes, cobalt complexed to MUX appears to remain in the +2 state (Storm & Dunn, 1985).

Binding to Preformed B10 Sites. The rate of association of Zn^{2+} to the B10 site (k_1) is comparable in magnitude with the association rate constants tabulated by Eigen and Wilkins (1964) for zinc binding to small molecules (Figure 3A). The Co^{2+} association rate measured for the B10 site (Figure 3B) is also very similar to k_1 values reported for the formation of Co^{2+}–small molecule complexes [compare the 3.5×10^5 M^{-1} s^{-1} value found here for Co^{2+} binding to the insulin hexamer with the second-order rate constant for formation of the cobalt–histidine complex, 3×10^5 M^{-1} s^{-1}, Eigen and Wilkins (1964)]. The similarities of the insulin rate constants to those of small molecule systems indicate that the rate-limiting step for binding of either Zn^{2+} or Co^{2+} to the B10 site very likely involves the removal of the first inner-sphere coordinated water molecule from the approaching metal ion. In contrast to Zn^{2+} and Co^{2+}, the binding of Cd^{2+} to the B10 site (Figure 3C) is unusually slow; in comparison to small molecule ligand exchange rates, the rate of association is at least 2 orders of magnitude slower than would be predicted if inner-sphere coordination is the rate-limiting step. Therefore, the rate-limiting step for Cd^{2+} binding must be some other process.

The X-ray structure of the zinc-bound B10 site shows the three His(B10) imidazole rings packed around the central zinc ion with little extra space. Zn^{2+} and Co^{2+} are similar in size (ionic radius 0.7 Å), while cadmium is much larger (ionic radius 1.0 Å). The X-ray structures of the metal ion free insulin hexamer and the Cd^{2+}-substituted hexamer (Dunn et al., 1987; C. Hill, Z. Dauter, M. F. Dunn, and G. G. Dodson, unpublished results) show that in both derivatives the N–N distance between imidazolyl ligands at the B10 site is nearly identical with that found in the two-zinc insulin hexamer structure. Since movement of the B10 imidazole rings is unnecessary for Cd^{2+} binding to occur to this structure, the event(s) that limits (limit) the rate of binding of Cd^{2+} to this site is (are) not obvious.

Binding of Limiting Metal Ion to Excess Metal-Free Insulin. From the stopped-flow study presented in Figure 4, it is clear that Zn^{2+}, Cd^{2+}, and Ca^{2+} are bound in extremely rapid events, while no such rapid process is detected with Co^{2+}. In light of the previously discussed specificity of the B10 site for these metal ions, the amounts bound and the association constants rule out the identification of the rapid (dead-time) event as the binding of metal ion to metal ion free hexamer (either preformed or rapidly formed during mixing). Since tetramer and dimer already preexist in significant amounts, binding to these species does not require a protein assembly step.

Of the preexisting species, monomer has no strong chelating sites, and thus it is unlikely to be the binding species. Dimer is present in high amounts but has only a single histidyl moiety at each B10 "site" position and only a single pair of carboxyl groups at each B13 position. It is possible that these carboxyls, which are quite close together and appear to be hydrogen bonded in the structures of dimeric dogfish insulin (Bajaj et al., 1983) and porcine 2Zn–insulin (Blundell et al., 1972), reorient and form a new metal ion binding site (Figure 1). However, there is no independent evidence indicating that this site competes with the crystallographically identified B13 site formed by the carboxyl pairs that bridge the dimer–dimer interface. The tetramer should contain one B13 site (across the dimer–dimer interface). Since for the conditions employed in Figure 4 the PB model (Figure 2) predicts a large amount of metal ion free tetramer (Table I), it appears that the B13 site is present in sufficient quantity to account for the amount of metal that disappears in the dead time. Note that all of the metal ions which bind in the dead time (Figure 4, Table I) also have been shown to bind at the hexamer B13 site by either crystallographic, NMR, or solution experiments (Blundell et al., 1972; Emdin et al., 1980; Sudmeier et al., 1981; Storm & Dunn, 1985; Dunn et al., 1987). Consequently, we conclude that the dead-time event is dominated by metal ion binding to the B13 sites of tetrameric insulin.

There exist several weak zinc-binding sites on the surface of the hexamer, most notably the Phe(B1)αNH_2–Glu(A17) carboxylate site between dimers. Contributions from this site also may be significant for the following reason: when zinc insulin crystals are soaked in excess zinc at pH 6.2, the B1–A17 sites have lower occupancies than do the B13 sites (indicating a lower affinity) (Emdin et al., 1980). However, higher pH should increase the affinity of this site via neutralization of the Phe(B1)αNH_3^+ ion. The tetramer also has two partially formed B10 sites, each involving two B10 histidyl moieties. Nevertheless, Co^{2+}, which has a strong preference for nitrogen ligands and therefore would be expected to bind more strongly to the partially formed B10 sites of tetrameric insulin than either Zn^{2+} or Cd^{2+}, does not give a rapid binding step. Therefore, under the conditions used, it appears that the participation of sites other than the tetramer B13 sites and possibly the Phe(B1)–Glu(A17) sites is negligible.

The calculated equilibrium constants for the dissociation of Zn^{2+} and Cd^{2+} from the tetramer B13 site (Figure 5) are similar in magnitude to the value of 4×10^{-6} M found for the binding of Cd^{2+} to the hexamer B13 site (Storm & Dunn, 1985). From the data presented in Figure 5, it appears that the addition of the third dimer unit contributes very little to the binding of these metal ions. In contrast, the dissociation constant for Ca^{2+} from the tetramer B13 site (estimated from several rapid kinetic and equilibrium spectrophotometric experiments in this study) is about 1×10^{-3} M, whereas for hexamer B13 sites the value drops to 8.3×10^{-5} M (Storm

& Dunn, 1985). Thus it appears that the assembly of hexamer from dimer and tetramer closes off the central cavity from the bulk solvent and increases the affinity for Ca^{2+} more than tenfold.

The association rates of Zn^{2+} and Cd^{2+} assigned to the tetramer B13 sites (Figure 5B) are consistent with the association rates of these metal ions to various small molecule ligands. The value for Zn^{2+}, 5×10^6 M^{-1} s^{-1}, is about the same as for the B10 site and, therefore, also appears to be limited by the removal of the first metal ion coordinated water molecule. The faster Cd^{2+} rate constant, 9×10^6 M^{-1} s^{-1}, probably is due to the larger ionic size of Cd^{2+} vis-ã-vis Zn^{2+}; the Cd^{2+} aqua complex coordinates water molecules less tightly, and ligand exchange occurs more rapidly. Although both the B10 and B13 sites probably have similar accessibility to solvent, the rate constant for Cd^{2+} binding to the tetramer B13 site is some 40 times faster than the rate constant for Cd^{2+} binding to hexameric B10 sites. This behavior indicates that water removal from the metal ion is not the rate-limiting step for Cd^{2+} binding to the hexamer B10 site.

When the accuracy of the rate estimations is taken into consideration, the dissociation constants calculated from the kinetic data are in reasonable agreement with the values obtained from the much more accurate amplitude data (Figure 5A). The dissociation constant for Cd^{2+}, 15 μM, is in good agreement with the 9 μM value found from amplitude data. The Zn^{2+} value, 56 μM, is larger than the 9 μM number found in the amplitude analysis and probably reflects the large uncertainties in rate estimations calculated by using only the final 10–12% of the entire time course.

In conclusion, the assembly of the zinc–insulin hexamer involves rate-limiting protein–protein association steps. The metal ion binding steps are relatively rapid processes. Via binding to the preformed Glu(B13) metal ion binding sites of the insulin tetramer, Ca^{2+} and Zn^{2+} drive assembly of the hexamer. Coordination of Zn^{2+} to the hexameric His(B10) sites provides additional thermodynamic stabilization.

Registry No. Zn, 7440-66-6; Co, 7440-48-4; Cd, 7440-43-9; Ca, 7440-70-2; insulin hexamer, 37243-75-7; insulin, 9004-10-8; insulin tetramer, 9066-40-4.

REFERENCES

Bajaj, M., Blundell, T. L., Pitts, J. E., Wood, S. P., Tatnell, M. A., Falkmer, S., Emdin, S. O., Gowan, L. K., Crow, H., Schwabe, C., Wollmer, A., & Strassburger, W. (1983) *Eur. J. Biochem. 135*, 535–542.

Baker, E. N., Blundell, T. L., Cutfield, J. F., Cutfield, S. M., Dodson, E. J., Dodson, G. G., Hodgkin, D. M. C., Hubbard, R. E., Isaacs, N. W., Reynolds, C. D., Sakabe, K., Sakabe, N., & Vijayan, N. M. (1988) *Philos. Trans. R. Soc. London, B* (in press).

Bentley, G. A., Dodson, E. J., Dodson, G. G., Hodgkin, D. C., & Mercola, D. A. (1976) *Nature (London) 261*, 166–168.

Bernasconi, C. F. (1976) in *Relaxation Kinetics*, p 13, Academic, New York.

Blundell, T., Dodson, G., Hodgkin, D., & Mercola, D. (1972) *Adv. Protein Chem. 26*, 279–402.

Bohidar, H. B., & Geissler, E. (1984) *Biopolymers 23*, 2407–2417.

Bradbury, J. H., Ramesh, V., & Dodson, G. (1981) *J. Mol. Biol. 150*, 609–613.

Brill, A. S., & Venable, J. H. (1968) *J. Mol. Biol. 36*, 343–353.

Dodson, E. J., Dodson, G. G., Hodgkin, D. C., & Reynolds, C. D. (1979) *Can. J. Biochem. 57*, 469–479.

Dunn, M. F., Palmieri, R., Kaarsholm, N. C., Roy, M., Lee, R. W.-K., Dauter, Z., Hill, C., & Dodson, G. G., (1987) in *Proceedings of the Fifth International Symposium on Calcium Binding Proteins in Health and Disease* (Norman, A. W., Vanaman, T. C., & Means, A., Eds.) pp 372–383, Academic, New York.

Eigen, M., & Wilkins, R. G. (1964) in *Mechanisms of Inorganic Reactions* (Gould, R. F., Ed.) pp 55–80, American Chemical Society, Washington, DC.

Emdin, S. O., Dodson, G., Cutfield, J. M., & Cutfield, S. M. (1980) *Diabetologia 19*, 174–182.

Fersht, A. (1985) in *Enzyme Structure and Mechanism*, 2nd ed., p 475, W. H. Freeman, New York.

Frank, B. H., & Veros, A. J. (1970) *Biochem. Biophys. Res. Commun. 38*, 284.

Frank, B. H., Pekar, A. H., & Veros, A. J. (1972) *Diabetes 21*, 486–491.

Fredericq, E. (1956) *Arch. Biochem. Biophys. 65*, 218–228.

Goldman, J., & Carpenter, F. H. (1974) *Biochemistry 13*, 4566–4574.

Grant, P. T., Coombs, T. L., & Frank, B. H. (1972) *Biochem. J. 126*, 433–440.

Holyer, R. H., Hubbard, C. D., Kettle, S. F. A., & Wilkins, R. G. (1966) *Inorg. Chem. 5*, 622–625.

Jeffrey, P. D., & Coates, J. H. (1966) *Biochemistry 5*, 489–498.

Jeffrey, P. D., Milthorpe, B. K., & Nichol, L. W. (1976) *Biochemistry 15*, 4660–4665.

Kaarsholm, N. C., & Dunn, M. F. (1987) *Biochemistry 26*, 883–890.

Kaplan, H., Chan, A. M. L., Oda, G., & Hefford, M. A. (1984) *Biochem. J. 217*, 135–143.

Koren, R., & Hammes, G. G. (1976) *Biochemistry 15*, 1165–1171.

Lord, R. S., Gubensek, F., & Rupley, J. A. (1973) *Biochemistry 12*, 4385–4392.

Milthorpe, B. K., Nickol, L. W., & Jeffrey, P. D. (1977) *Biochim. Biophys. Acta 495*, 195–202.

Palmieri, R., Lee, R. W.-K., & Dunn, M. F. (1988) *Biochemistry 27*, 3387–3397.

Peking Insulin Structure Research Group (1974) *Sci. Sin. 17*, 779–792.

Pocker, Y., & Biswas, S. B. (1980) *Biochemistry 19*, 5043–5049.

Pocker, Y., & Biswas, S. B. (1981) *Biochemistry 20*, 4354–4361.

Porter, R. R. (1953) *Biochem. J. 53*, 320–328.

Roy, M., Lee, R., & Dunn, M. F. (1987) in *Calcium-Binding Proteins in Health and Disease* (Norman, A. W., Vanaman, T. C., & Means, A., Eds.) pp 424–426, Academic, New York.

Rupley, J. A., Renthal, R. D., & Praissman, M. (1967) *Biochim. Biophys. Acta 140*, 185–187.

Sakabe, N., Sakabe, K., & Sasaki, K. (1981) in *Structural Studies on Molecules of Biological Interest* (Dodson, G., Glusker, J. P., & Sayre, D., Eds.) pp 509–526, Clarendon Press and Oxford University Press, London.

Scarpa, A., Brinley, F. J., & Dubyak, G. (1978) *Biochemistry 17*, 1378–1386.

Schicktkrull, J. (1956) *Acta Chem. Scand. 10*, 1455–1458.

Smith, G. D., Swenson, D. C., Dodson, E. J., Dodson, G. G., & Reynolds, C. D. (1984) *Proc. Natl. Acad. Sci. U.S.A. 81*, 7093–7097.

Storm, M. C., & Dunn, M. F. (1985) *Biochemistry 24*, 1749–1756.
Strazza, S., Hunter, R., Walker, E., & Darnall, D. W. (1985) *Arch. Biochem. Biophys. 238*, 30–42.
Sudmeier, J. L., Bell, S. J., Storm, M. C., & Dunn, M. F. (1981) *Science (Washington, D.C.) 212*, 560–562.
Williamson, K. L., & Williams, R. J. P. (1979) *Biochemistry 18*, 5966–5972.

^{31}P NMR Magnetization-Transfer Measurements of Flux between Inorganic Phosphate and Adenosine 5′-Triphosphate in Yeast Cells Genetically Modified To Overproduce Phosphoglycerate Kinase†

Kevin M. Brindle
Department of Biochemistry, University of Oxford, South Parks Road, Oxford OX1 3QU, England
Received November 13, 1987; Revised Manuscript Received March 17, 1988

ABSTRACT: ^{31}P NMR magnetization-transfer measurements were used to measure flux between inorganic phosphate and ATP in the reactions catalyzed by phosphoglycerate kinase and glyceraldehyde-3-phosphate dehydrogenase in anaerobic cells of the yeast *Saccharomyces cerevisiae*. Flux between ATP and P_i and glucose consumption and ethanol production were measured in cells expressing different levels of phosphoglycerate kinase activity. Overexpression of the enzyme was obtained by transforming the cells with a multicopy plasmid containing the phosphoglycerate kinase coding sequence and portions of the promoter element. Fluxes were also measured in cells in which the glyceraldehyde-3-phosphate dehydrogenase activity had been lowered by limited incubation with iodoacetate. These measurements showed that both enzymes have low flux control coefficients for glycolysis but that phosphoglycerate kinase has a relatively high flux control coefficient for the ATP ↔ P_i exchange catalyzed by the two enzymes. The P_i ↔ ATP exchange velocities observed in the cell were shown to be similar to those displayed by the isolated enzymes in vitro under conditions designed to mimic those in the cell with respect to the enzyme substrate concentrations.

Extrapolation of enzyme kinetic data obtained in vitro to the intact cell assumes a detailed knowledge of the intracellular environment in terms of the enzyme's substrate concentrations and the levels of various effectors and other factors which may influence the enzyme's activity. An important feature of the intracellular environment is the relatively high protein concentration. This can have a number of consequences; for example, the free concentration of an enzyme's substrates may be much less than the total extractable concentration if there is binding of the substrate to other enzymes and cell proteins [see Sols and Marco (1970) for review]. High enzyme concentrations may also result in enzyme–enzyme interactions which are not observed at the relatively low concentrations used for determination of steady-state kinetics in vitro (Srivastava & Bernhard, 1986a,b). There is continued interest, for example, in the hypothesis that the enzymes of a metabolic pathway may associate to form a multienzyme complex [see Srere (1987) for review]. Complex formation, it is suggested, can result in "channeling" of substrates within the complex leading to an increase in the rate of the coupled reactions. Indeed, it has been shown that coimmobilization of the glycolytic enzymes can result in an enormous increase in the rate of reaction compared with that observed with the same concentrations of enzymes free in solution (DeLuca & Krika, 1983). Some of the best evidence for complex formation among the glycolytic enzymes in vivo has come from studies showing specific interactions between sequential pairs of glycolytic enzymes and interactions between the glycolytic enzymes and other cellular proteins (Srivastava & Bernhard, 1986a,b; Srere, 1987). An interaction has been observed, for example, between glyceraldehyde-3-phosphate dehydrogenase and phosphoglycerate kinase which results in direct transfer of 1,3-diphosphoglycerate from one enzyme active site to the other, resulting in a substantial increase in the rate of the coupled reaction (Weber & Bernhard, 1982). There have also been numerous studies on the association of glycolytic enzymes with the band 3 protein of the erythrocyte membrane. Whether this interaction occurs in vivo is not clear since binding is only observed under conditions of low ionic strength in vitro. We investigated the binding of glyceraldehyde-3-phosphate dehydrogenase to the band 3 protein in the human erythrocyte by comparing the activity expressed by the enzyme in the cell with the activity expressed by the isolated enzyme in vitro, when free and when bound to the band 3 protein (Brindle et al., 1982). Enzyme activity in vivo was measured by using ^{1}H NMR to monitor noninvasively a coupled ^{1}H/^{2}H exchange reaction in which the enzyme was involved. The study showed that the enzyme was totally inhibited when bound to band 3 and that the activity expressed by the enzyme in the cell was too high for there to be any significant binding of the enzyme to the membrane. This strategy of comparing the kinetic properties expressed by an enzyme in vivo and in vitro has been used here to seek evidence for glycolytic enzyme complex formation in the yeast *Saccharomyces cerevisiae*. Since glycolytic flux can be very high in yeast, we would expect a glycolytic enzyme complex, if its exists, to be evident in this organism.

The enzymes investigated in this study, phosphoglycerate kinase (PGK)[1] and glyceraldehyde-3-phosphate dehydrogenase

† This work was supported by the Medical Research Council of Great Britain and the Royal Society.

0006-2960/88/0427-6187$01.50/0